JOURNAL OF QUATERNARY SCIENCE (2020) **35**(7) 961–973 ISSN 0267-8179. DOI: 10.1002/jqs.3236

JQS Journal of Quaternary Science QRA Quaternary Research Association

The new ^{14}C chronology for the Palaeolithic site of La Ferrassie, France: the disappearance of Neanderthals and the arrival of *Homo sapiens* in France

S. TALAMO,[1,2]* V. ALDEIAS,[1,3] P. GOLDBERG,[4,5] L. CHIOTTI,[6] H. L. DIBBLE,[1,7,8] G. GUÉRIN,[9] J.-J. HUBLIN,[1,10] S. MADELAINE,[11,12] R. MARIA,[1,13] D. SANDGATHE,[14,15] T. E. STEELE,[1,16] A. TURQ[11,12] and S. J. P. MCPHERRON[1]

[1]Department of Human Evolution, Max Planck Institute for Evolutionary Anthropology, Deutscher Platz 6, Leipzig, 04103, Germany
[2]Department of Chemistry G. Ciamician, Alma Mater Studiorum, University of Bologna Via Selmi 2, Bologna, 40126, Italy
[3]Interdisciplinary Center for Archaeology and Evolution of Human Behavior, University of Algarve, Campus Gambelas Edificio 1, Faro, 8005-139, Portugal
[4]CAS, SEALS, University of Wollongong, Northfields Avenue, Wollongong NSW, 2522, Australia
[5]Institute for Archaeological Sciences, University of Tübingen, Rümelinstr. 23, Tübingen, 72070, Germany
[6]Département Homme et Environnement, Muséum national d'Histoire Naturelle, UMR 7194 du CNRS, Abri Pataud, 24620 Les Eyzies-de-Tayac, France
[7]Department of Anthropology, University of Pennsylvania, Philadelphia, USA
[8]Institute for Human Origins, Arizona State University, USA
[9]IRAMAT-CRP2A, UMR 5060 CNRS - Université Bordeaux Montaigne e Maison de l'archéologie, Esplanade des Antilles, Pessac, 33600, France
[10]Collège de France, 11, place Marcelin Berthelot, 75005, Paris, France
[11]Univ. Bordeaux, CNRS, Ministère de la Culture et de la Communication, PACEA UMR 5199, Allée Geoffroy Saint-Hilaire, FR-, Pessac, 33615, France
[12]Musée national de Préhistoire, F-24620 Les Eyzies-de-Tayac, France
[13]Department of Structural Biology, Weizmann Institute of Science, Rehovot, Israel
[14]Department of Archaeology, Simon Fraser University, Burnaby, Canada
[15]University of Pennsylvania Museum of Archaeology and Anthropology, Pennsylvania, USA
[16]Department of Anthropology, University of California, Davis, Davis, California, 95616 USA

Received 26 February 2020; Revised 21 July 2020; Accepted 24 July 2020

ABSTRACT: The *grand abri* at La Ferrassie (France) has been a key site for Palaeolithic research since the early part of the 20th century. It became the eponymous site for one variant of Middle Palaeolithic stone tools, and its sequence was used to define stages of the Aurignacian, an early phase of the Upper Palaeolithic. Several Neanderthal remains, including two relatively intact skeletons, make it one of the most important sites for the study of Neanderthal morphology and one of the more important data sets when discussing the Neanderthal treatment of the dead. However, the site has remained essentially undated. Our goal here is to provide a robust chronological framework of the La Ferrassie sequence to be used for broad regional models about human behaviour during the late Middle to Upper Palaeolithic periods. To achieve this goal, we used a combination of modern excavation methods, extensive geoarchaeological analyses, and radiocarbon dating. If we accept that Neanderthals were responsible for the Châtelperronian, then our results suggest an overlap of ca. 1600 years with the newly arrived *Homo sapiens* found elsewhere in France. © 2020 The Authors. *Journal of Quaternary Science* Published by John Wiley & Sons Ltd

KEYWORDS: chronology; human evolution; La Ferrassie; Palaeolithic; radiocarbon

Introduction

In Europe, the period between 50 000 and 39 000 years ago was particularly important for Neanderthals and their interaction with *Homo sapiens* (Hublin, 2015, Higham *et al.*, 2014, Hublin *et al.*, 2020). During this time, usually referred to as the Middle to Upper Palaeolithic transition period, *Homo sapiens* entered Europe and eventually spread across most of the continent, encountering Neanderthals along the way. By the end of this period, *Homo sapiens* had replaced Neanderthals but carried with them genetic evidence of interactions with Neanderthals (Fu *et al.*, 2015). Additionally, in many regions, artefact assemblages from this period are also interpreted as transitional industries. These relatively short-lived and spatially limited archaeological entities appear to combine elements of the preceding Middle Palaeolithic (Neanderthals) with innovative elements of the subsequent Upper Palaeolithic (*Homo sapiens*), though to varying degrees (Ruebens *et al.*, 2015). Who made the so-called transitional industries? To what extent were late Neanderthal behavioural innovations influenced by incoming *Homo sapiens*? and How frequently did one group encounter the other? are questions that remain largely unresolved. The region-by-region timing of the spread of *Homo sapiens* and the demise of Neanderthals are all highly debated topics for which having good chronological control is essential (Hublin, 2015).

*Correspondence: S. TALAMO, as above.
E-mail: sahra.talamo@unibo.it

For the archaeological record of the last 50 000 years, AMS radiocarbon dating remains an essential tool for chronological reconstructions. However, its application to the transition period has been complicated by a number of factors: 1) the resolution of the calibration curve is still not accurate enough in this time range; 2) counting errors, which occur with any ^{14}C date, are greater for older ages and when combined with point 1 produce wide confidence intervals; 3) many of the key sites were excavated before and during the first half of the 20th century when excavators were less conscientious about documenting complicated stratigraphies and post-depositional movements of objects, further increasing the uncertainty associated with ^{14}C ages; and 4) while increasing the number of dated samples can help reduce these uncertainties, its destructive nature and its costs in archaeological budgets limit the number of dated materials in most contexts. While the radiocarbon community is constantly working to refine the calibration curve (Adolphi *et al.*, 2017, Muscheler *et al.*, 2014), here we provide a high-resolution chronology for the site of La Ferrassie (France). Recent excavations included extensive radiocarbon sampling ($n = 40$), which resulted in a collection of new ^{14}C dates and a new interpretation described below.

The site of La Ferrassie

The site of La Ferrassie is located on a small tributary of the Vézère river not far from the town of Le Bugue, France, (44° 57′ 06″ N, 00° 56′ 17″ E; 120 m asl). It consists of several localities, of which the best known is the so-called main shelter (the *grand abri*, hereafter La Ferrassie), where excavations were carried out in the early part of the 20th century by Capitan and Peyrony and in the 1960s and early 1970s by Delporte (Delporte and Delibrias, 1984; Peyrony, 1934) (Fig. 1).

La Ferrassie is the eponymous site for one particular variant of the Middle Palaeolithic, the Ferrassie Mousterian (Bordes, 1961), characterised by elevated proportions of scrapers and Levallois techniques of blank production. The La Ferrassie sequence was used to define stages of the Aurignacian (Delporte, 1984; Djindjian, 1986; de Sonneville-Bordes, 1960), a variant of the Upper Palaeolithic, and because of the number of Neanderthal individuals represented and their find context, the site has figured prominently in debates concerning Neanderthal burial and associated rituals (Smirnov, 1989; Zilhão, 2016).

The new excavations at La Ferrassie, led by one of the co-authors (A.T.) and conducted from 2010 to 2015, revised the stratigraphy and resampled the initial (1909) sections left by Capitan and Peyrony in the western sector of the site (Fig. 1) (Turq *et al.*, 2012; Guérin *et al.*, 2015). The revised stratigraphy is summarised in Table 1. The lowermost layers (1 to 5 of the new stratigraphy) contain Middle Palaeolithic stone tools (Dibble *et al.* 2018) associated with mostly large bovids (*Bison/Bos*) and red deer (*Cervus elaphus*). These levels are overlain by a well-constrained Châtelperronian in Layer 6, with Châtelperron points, and a bladelet component. The overlying Layer 7 is subdivided into 7a and 7b. Layer 7a contains diagnostic Aurignacian artefacts (Table 1) and is characterised by the presence of carinated scrapers and a few, but very characteristic, Aurignacian blades. The production of wide and robust blades also characterises this industry as an Early Aurignacian. Layer 7b has mixed components: the presence of Aurignacian retouch is characteristic of the Early Aurignacian, whereas nose-ended scrapers and very regular small Dufour bladelets are compatible with the Recent Aurignacian. Reindeer (*Rangifer tarandus*) dominate in both Layers 6 and 7. Due mainly to the limited extent over which they could be excavated, Layers 8 and 9 are still poorly understood both in terms of their formation processes and their archaeological affinities. Nevertheless, Layer 8 contains a mix of Aurignacian and Gravettian, and Layer 9 could be attributed to the Gravettian.

Though the dates presented here come from the Western Sector of the site, new excavations also took place towards the east, in what we call the Northern Sector and where Delporte previously excavated and found another partial skeleton (LF 8 (Gómez-Olivencia *et al.*, 2015)). In this area of the site, the cultural sequence is similar to the Eastern and Western Sectors in that the Middle Palaeolithic, Châtelperronian and Upper Palaeolithic are all represented. However, it is important to emphasise that despite the similarities of the archaeological sequences, there is at present no direct physical correlation between the Northern and Western Sectors. Moreover, different and virtually independent depositional processes and mechanisms existed across the east–west length of the site (Goldberg *et al.*, 2016, Aldeias *et al.*, 2014).

Geology of the site

Though the site today has the appearance of a shelter (and was called le grand abri) we now know that it is part of an elongated karstic system whose breech in the roof gives the appearance of its being a shelter. We also know that the geology and stratigraphy at La Ferrassie are complex and quite variable across the site. This assertion is based on a comparison of our section in the Western Sector with the sections published by Peyrony (1934), the large section visible today in the Eastern Sector of the site (Delporte and Delibrias, 1984; Texier, 2006), some small test excavations we did between the East and West Sectors, and work we did in the Northern Sector. As a result, though the Western, Northern and Eastern sectors of the site share similar archaeological sequences–although the numbering and differentiation of layers are different–their depositional sequences must be considered independently. Here we focus on the Western Sector, which was the subject of our excavations and the new radiocarbon dating programme.

The stratigraphic descriptions and profiles published by Peyrony (1934) are rather rudimentary, and their exact equivalence to our profiles is not straightforward; although there is some semblance to his western profile, it is not similar to his is 1934 profile. However, based on one of his profiles which is the closest to our own excavations, a general correlation is possible (main text Table 1). This correlation with Peyrony's excavations covers the majority of our sequence (Layers 1–7); the overlying Layers 8–9 are particularly poorly represented here, and their Peyrony correlates are not clear.

The sequence in the Western Sector (Turq *et al.*, 2012, Guérin *et al.*, 2015) exhibits clear changes in lithologies and environments of deposition from the bottom to top. The basal red sandy layers (Layer 1) are waterlain and accumulated at the cave entrance by a small stream oriented NW–SE. The sedimentology and mode of deposition change abruptly with the onset of the overlying deposits. Layer 2 consists predominantly of yellow partly cemented, calcareous sand, rich in limestone éboulis that accumulated under markedly cold conditions, with cryoturbation and solifluction lobes that originated from limestone masses (old roof fall) situated to the west of the current excavation, at the location of the present-day road. It appears to have accumulated by a combination of roof fall, disaggregated quartz and limestone sand from the bedrock, and localised colluvial deposition of centimetre-sized rounded limestone fragments.

Layer 3, consisting of poorly sorted, silty, coarse to medium sand, fills in the lobate surface relief on the top of soliflucted

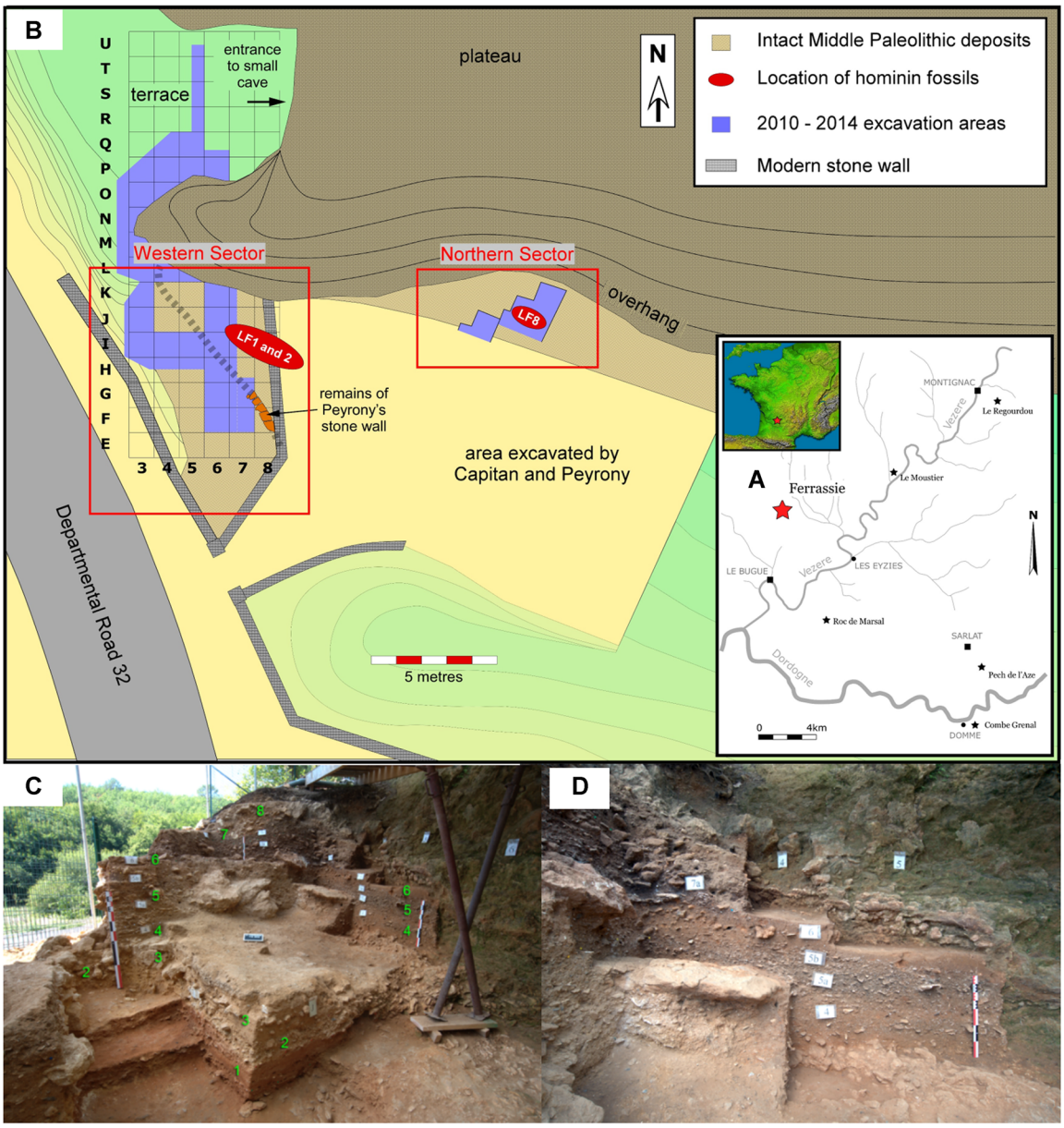

Figure 1. Location, stratigraphic sequence and the plan of La Ferrassie. (A) Location of the site in the department of Dordogne, France. (B) Plan view of the site. The square rows E through M represent the Grand Abri excavations. The remaining excavation squares are in front of the cave. (C) La Ferrassie, the northwestern part of the Western Sector looking W and NW along the I line. Stratigraphic units are indicated in green. (D) The northern part of the Western Sector showing deposits at the end of the 2013 season. Although this profile is close to the wall, notice the gradual contact between Layers 4 and 5a in the centre. The two upper tags '4' and '5' refer to square names and not to layers. [Color figure can be viewed at wileyonlinelibrary.com]

Layer 2, but overall it is rather horizontal and thickens slightly to the SE, following the sloping topographic surface of Layer 2. It appears to have accumulated by a combination of roof fall, disaggregated quartz and limestone sand from the bedrock, and localised colluvial deposition of centimetre-sized rounded limestone fragments.

Above Layer 3, the style of sedimentation begins to change. Layer 4 overlies Layer 3 with a distinct, locally sharp contact and is comprised of massive, compact silty medium sand with relatively abundant centimetre-sized pieces of bone and chert; highly fragmented burned bones occur in addition to what appear to be the remnants of a small (~ 1 cm across) combustion area. Along the West Profile, Layer 4 overlies a concentration of decimetre-sized roof fall blocks that is sandwiched between Layers 3 and 4. Stratigraphically upward, the inclination of Layer 4 increases radially away from the NW part of the site and is thicker there. In addition, thin section observations show that Layer 4 deposits–particularly along with the North profile–are weakly bedded and accumulated as colluvium. The inference is that after the initial accumulation of Layer 4, the large blocks of roof fall created a certain relief and at the same time, focused the deposits away from a virtual point source: a colluvial fan emanating from beyond the Western Profile, at a location which no longer exists (destroyed during road construction) but would have been situated along the modern road.

Layer 5, composed of reddish yellow pebbly silty sand with generally platy éboulis and abundant bone fragments, appears to represent the same type of deposit as Layer 4, although it is relatively richer in anthropogenic material (bones and lithics) and interstitial silt. It is clearly bedded with clasts dipping toward the east and following the inclination of the colluvial cone. Layer 5 grades upward from Layer 4 without a sharp contact.

Layer 6 is a rather uniform sandy layer near the north wall (the limestone cliff face) but stonier as followed across to the western section. It conformably rests on top of Layer 5 with a sharp contact. Its sandiness is a result of decalcification of

Table 1. Summary of the lithostratigraphy of La Ferrassie deposits exposed in the recent excavations.

Layer	Peyrony, 1934	Lithological description	Lithic industry	Interpretation
9	--	Cm-thick spatially restricted sandy deposit occurring in patches on bedrock sill in front of the Upper Cave; partly cemented, mottled light brown silty quartz sand with many calcitic roots.	Gravettian	Patches of sediments remaining from previous excavations
8	I	A gravelly channel deposit that truncates much of Layer 7; it is best exposed in the northwest corner of the excavation. It is a poorly sorted mixture of mm-sized rounded pebbles and cm-sized platy clasts of limestone.	Melding of Aurignacian and Gravettian	Fills steep-sided channels derived from the platform above
7	H, G, F	Compact, brown calcareous sandy silt with abundant lithics and bone. In the NW corner of the excavation, the upper part has been truncated by the gravelly channel deposit of Layer 8. The contact with Layer 6 below is irregular and distinct. As with Layers 5 and 6, the cone morphology of the deposits is reflected by dips to the southeast.	Aurignacian	Dry fall talus cone emanating from a platform above present-day road
6	E	A distinct sharp boundary with Layer 5 and along the north wall is compact massive strong brown, non-calcareous silty fine sand with some mica. A few angular clasts of éboulis occur at the top, along with scatters of flint and bone, some of which are calcined. It is well defined along the north wall but more difficult to delineate along the NW and Western parts of the excavation, where it is much more calcareous and not as well sorted. The dips are the same as those in Layer 5, with an overall inclination to the SE.	Châtelperronian	• Start of major anthropogenic inputs from Layer 3 upwards with few poorly preserved combustion features • Major roof fall events • In the middle of Layer 4, sediment source mainly upslope from NW from dry talus (Layers 3 to 6) • Dips increase slightly but visibly from Layer 4 to 6
5	D	Varies in thickness from ~ 50 cm in the west to ~30 cm along the north wall, a result of decalcification along the north wall: In the western part of the excavation, it is composed of reddish yellow pebbly silty sand with generally platy limestone and abundant bone fragments. Like Layer 4, it is partially decalcified and thus richer in quartz sand, but rich in flints and burnt bone in the fine fraction. Layer 5 has different dip directions: in the North part of the excavation, the apparent dip is to the east, whereas in the Western part, it dips to the SSE. These differences in dip are interpreted as differently oriented sections of a sedimentary cone whose apex was situated in the area above what is now part of the road and now no longer present.	Mousterian	
4	C	Only partially exposed due to removal by Peyrony. In the western excavations, Layer 4 is massive, compact silty medium sand with relatively abundant cm-sized pieces of bone and flint. Against the northern wall of the excavation where decalcification is marked, it is sandier, and impoverished in limestone fragments but still rich in flints and burnt bone.	Mousterian	
3	—	Yellow, poorly sorted silty, coarse to medium sand, punctuated by rounded, cm- to dm-sized blocks of limestone and roof fall that occurs in the westernmost part of the excavations.	Mousterian	
2	B	Yellow, partly cemented, calcareous sand; in the west, rich in rock fragments and limestone blocks (cm to dm in size). Marked ice-lensing.	Mousterian with bifaces	Rockfall and its physical breakdown products during a marked cold phase
1	A	Predominantly red, poorly sorted sand, locally exhibiting beds and thin lenses of cm-sized rock fragments, and pockets and stringers of well-rounded, mm- to cm-sized iron grains. The top of Layer 1 is undulating and irregular, and it has incorporated some of the overlying yellower sediment of Layer 2, resulting in a more gradational contact.	Mousterian with bifaces	Water lain deposits reworked from surrounding red siliceous materials (Tertiary *altérite;* residual phreatic deposits)

sediments along the north wall, while along the western section it is enriched in rounded gravels derived from the Upper Cave at La Ferrassie.

Layer 7 overlies Layer 6 with a clear, somewhat gradational contact, though the lithologies are strikingly different. The dips of the deposits follow those of the underlying layers.

In sum, from a geological point of view, the upper part of Layer 4 through the deposition of Layer 7 constitute a similar sequence of colluvial cone deposits with no apparent unconformities or gaps recorded within or between the individual layers.

Previous radiocarbon dating at La Ferrassie

Since 1984, there have been several efforts to apply radiocarbon dating to the La Ferrassie sequence.

Previously, a set of radiocarbon dates for the Eastern Sector of La Ferrassie was published by Delibrias (1984) and then followed by Mellars *et al.* (1987). After re-evaluating the ultrafiltration step (Higham, 2011; Higham *et al.*, 2006; Brown *et al.*, 1988), re-analyses on two animal bone samples from Delporte's excavation (Delporte and Delibrias, 1984) confirmed the advantage of using the ultrafilter and provided the only reliable radiocarbon-based dates for the site. While the two new dates provided by Higham and collaborators (Higham *et al.*, 2006) are not sufficient to build a chronology of the deposits, when combined with the data set coming from the previous excavation seasons, they do show that there is no agreement between the whole data set and the stratigraphy established by Delporte (Fig. 14 in Bertran *et al.*, 2008). Overall, the ages display considerable scatter, likely due to the inadequate removal of modern ^{14}C contamination (as is demonstrated in Higham *et al.* (2006)), as well as possible stratigraphic and/or sample provenience issues.

More recently, an attempt was also made to directly date the LF 1 Neanderthal skeleton using ^{14}C (Higham *et al.*, 2014 in SI). Unfortunately, here too there was a serious problem with modern contamination, and different ages were obtained from different pretreatment methods applied to two different bones presumed to be from the same individual. The distal right tibia dated to around 12 000 years ^{14}C BP while the distal left tibia could be as old as 35 000 ^{14}C BP. These different results led Higham and collaborators to conclude that proteinaceous contaminants made LF 1 impossible to directly date (Higham *et al.*, 2014).

The first successful attempt to provide ages for the sequence came from luminescence dating (optically stimulated luminescence, OSL, of quartz and infra-red stimulated luminescence, IRSL, of feldspar) (Guérin *et al.*, 2015, Frouin *et al.*, 2017a). These ages are stratigraphically consistent and show that the base of the deposits (Layers 1 and 2) are associated with late MIS 5 to MIS 4 and are outside the range of radiocarbon dating. The OSL ages also show that most of the sequence (Layers 3 to 7) is relatively recent (55 ka and younger) (Table 2).

Table 2. Optically stimulated luminescence (OSL) ages published in Guérin *et al.* (2015) from Layers 7 to 3.

Level	Sample numbers	OSL age	1σ err
Layer 7	FER 1	37 200	1900
Layer 6	FER 2	42 200	2900
Layer 5	FER 4	45 300	2800
Layer 5	FER 14	43 100	2600
Layer 5	FER 3	39 700	2300
Layer 4	FER 6	54 300	3500
Layer 4	FER 5	44 400	2600
Layer 3	FER 8	51 500	2700
Layer 3	FER 13	44 300	2500
Layer 3	FER 7	56 600	3000

Material and methods

Sample selection

We applied radiocarbon dating to 40 animal bone samples from the Middle Palaeolithic (Layers 2–5), the Châtelperronian (Layer 6), and the Upper Palaeolithic (Layers 7, 8 and 9) (Table 3) to further refine the La Ferrassie chronology (Figs. 2 and 3). Of the 40 samples, 18 had indications of human modification, such as butchery (cut and scraping marks) or use as bone retouchers. The other 22 did not show human modifications and were selected in part to test whether bones with and without human modifications would give different ages as an additional insight into possible site formation processes. Sample selection also took into account the spatial distribution of all samples.

Radiocarbon sample pretreatment and collagen quality control

All bone samples were pretreated in the Department of Human Evolution at the Max Planck Institute for Evolutionary Anthropology (MPI-EVA), Leipzig, Germany, using the method described by Talamo and Richards (2011): the outer surface of the bone sample is first cleaned by a shot blaster and then 500 mg of the bone is taken. The samples are then decalcified in 0.5 M HCl at room temperature until no CO_2 effervescence is observed. 0.1 M NaOH is added for 30 min to remove humics. The NaOH step is followed by a final 0.5 M HCl step for 15 min. The resulting solid is gelatinised following Longin (1971) at pH 3 in a heater block at 75°C for 20 h. The gelatine is then filtered in an Eeze-Filter (Elkay Laboratory Products (UK) Ltd.) to remove small (>80 μm) particles. The gelatine is then ultrafiltered (Brown *et al.*, 1988) with Sartorius 'Vivaspin Turbo' 30 KDa ultrafilters. Prior to use, the filter is cleaned to remove carbon containing humectants (Brock *et al.*, 2007). The samples are lyophilised for 48 h. In order to monitor contamination introduced during the pretreatment stage, a sample from a cave bear bone, kindly provided by D. Döppes (MAMS, Germany), was extracted along with the batch of La Ferrassie samples (Korlević *et al.*, 2018).

To assess the preservation of the collagen yield, C:N ratios, together with isotopic values, are evaluated. The C:N ratio should be between 2.9 and 3.6 and the collagen yield not less than 1% of the weight (van Klinken, 1999). The stable isotopic analysis was carried out at the MPI-EVA (Lab Code S-EVA) using a ThermoFinnigan Flash EA coupled to a Delta V isotope ratio mass spectrometer. In addition to the C:N ratio, we evaluated the quality of the collagen using Fourier transform infrared spectrometry (FTIR) (D'Elia *et al.*, 2007). FTIR was used to check for the presence of the three major characteristic peaks of collagen; specifically, the bands at around 1660 cm^{-1} (amide I), 1550 cm^{-1} (amide II) and 1450 cm^{-1} (amino acid proline absorption) that can be mainly attributed to (ν(C = O)), (ν(C-N)) and (δ(CH2)) vibrations, respectively (Fig. S1) (D'Elia *et al.*, 2007, Yizhaq *et al.*, 2005). About 0.3 mg of sample was homogenised in an agate mortar and pestle, then mixed with ~40 mg of IR grade KBr powder and pressed into a pellet using a manual hydraulic press (Wasserman). Spectra were recorded in transmission mode with an Agilent 660 FTIR Spectrometer (Agilent Technologies) with a DTGS detector, at 4 cm^{-1} resolution and averaging of 32 scans between 4000 and 400 cm^{-1} using Resolution Pro software (Agilent Technologies).

Table 3. Radiocarbon dates, isotopic values, % of collagen and C:N ratios of La Ferrassie.

MPI Code	Square-ID Number	Layer	Archaeological attribution	Taxa	% Coll	C:N	Year	AMS No.	^{14}C Age	1σ Err	Depth (Z)
S-EVA 31841	M3-8	9	Under Study	unknown	2.3	3.2	2015	MAMS-25529	27 070	150	0.436
S-EVA 31846	M3-306	9	Under Study	*Cervus/Rangifer*	2.1	3.3	2015	MAMS-25530	25 120	120	0.383
S-EVA 31836	M3-426	8	Under Study	unknown	2.1	3.3	2015	MAMS-25527	26 270	130	0.185
S-EVA 31840	M3-479	8	Under Study	unknown	2.3	3.4	2015	MAMS-25528	27 160	150	0.113
S-EVA-26879	L5-204	•7	Aurignacian	unknown	1.6	3.2	2013	MAMS-17584	35 206	160	-1.066
S-EVA-26517*	I3-391	7	Aurignacian	unknown	1.8	3.2	2012	MAMS-16376	33 090	240	-0.916
S-EVA-26513	L4-661	7	Aurignacian	unknown	2.0	3.2	2012	MAMS-16375	32 250	230	-0.910
S-EVA 31805	K3-2369	7	Aurignacian	unknown	2.4	3.2	2015	MAMS-25520	33 100	260	-0.883
S-EVA 31806*	K3-2402	7	Aurignacian	unknown	2.2	3.2	2015	MAMS-25521	32 510	240	-0.875
S-EVA-26511*	L4-484	7	Aurignacian	*Cervus/Rangifer*	1.6	3.2	2012	MAMS-16374	32 610	230	-0.871
S-EVA-26519*	J2-313	7	Aurignacian	unknown	2.6	3.3	2012	MAMS-16377	32 980	240	-0.868
S-EVA 31831	I3-560	7	Aurignacian	*Rangifer*	2.4	3.3	2015	MAMS-25526	33 730	290	-0.747
S-EVA 31827	J3-160	7	Aurignacian	unknown	2.2	3.3	2015	MAMS-25525	32 810	270	-0.737
S-EVA-26510	I4-219	6	Châtelperronian	unknown	2.5	3.2	2012	MAMS-16373	37 380	390	-1.195
S-EVA-26880	L5-237	•6	Châtelperronian	unknown	1.1	3.3	2013	MAMS-17585	32 450	130	-1.182
S-EVA-29452*	L4-1189	•6	Châtelperronian	unknown	1.3	3.3	2014	MAMS-21207	38 910	390	-1.126
S-EVA 31816	K3-3204	6	Châtelperronian	*Equus*	2.0	3.3	2015	MAMS-25522	36 590	390	-1.052
S-EVA 31818	K3-3184	6	Châtelperronian	unknown	2.4	3.2	2015	MAMS-25523	39 000	510	-1.047
S-EVA-29453*	L4-1630	•6	Châtelperronian	*Rangifer*	1.1	3.2	2014	MAMS-21208	36 300	300	-1.011
S-EVA 31819	K3-2953	6	Châtelperronian	unknown	2.6	3.2	2015	MAMS-25524	40 770	650	-1.009
S-EVA-29451*	L3-926	6	Châtelperronian	unknown	3.0	3.2	2014	MAMS-21206	40 890	500	-0.970
S-EVA-26873	I4-890	5	Middle Palaeolithic/Mousterian	unknown	2.6	3.2	2013	MAMS-17580	41 680	310	-1.473
S-EVA-26875*	J4-43	5	Middle Palaeolithic/Mousterian	large ungulate	2.3	3.2	2013	MAMS-17582	43 520	380	-1.448
S-EVA-26874*	I4-832	5	Middle Palaeolithic/Mousterian	unknown	2.8	3.2	2013	MAMS-17581	42 360	330	-1.424
S-EVA-26508	I4-709	5	Middle Palaeolithic/Mousterian	unknown	4.4	3.3	2012	MAMS-16372	42 370	680	-1.346
S-EVA-26507*	I4-666	5	Middle Palaeolithic/Mousterian	unknown	4.2	3.2	2012	MAMS-16371	42 150	660	-1.343
S-EVA-26506*	I4-423	5	Middle Palaeolithic/Mousterian	unknown	2.9	3.2	2012	MAMS-16381	43 370	300	-1.296
S-EVA-29455	L5-334	•5	Middle Palaeolithic/Mousterian	unknown	1.2	3.3	2014	MAMS-21209	39 740	430	-1.247
S-EVA-26877	I4-220	5	Middle Palaeolithic/Mousterian	unknown	3.1	3.2	2013	MAMS-17583	42 010	310	-1.202
S-EVA-29448*	I5-62	4	Middle Palaeolithic/Mousterian	unknown	2.7	3.2	2014	MAMS-21204	40 970	500	-1.974
S-EVA-29443*	I5-13	4	Middle Palaeolithic/Mousterian	unknown	1.8	3.4	2014	MAMS-21198	39 980	440	-1.930
S-EVA-29446*	I5-4	4	Middle Palaeolithic/Mousterian	unknown	3.9	3.2	2014	MAMS-21203	41 400	520	-1.864
S-EVA 31796*	I3-2260	4	Middle Palaeolithic/Mousterian	unknown	2.6	3.2	2015	MAMS-25518	40 220	590	-1.860
S-EVA-29450*	K6-172	•4	Middle Palaeolithic/Mousterian	large ungulate	4.3	3.3	2014	MAMS-21205	38 050	360	-1.808
S-EVA 31785	J4-94	4	Middle Palaeolithic/Mousterian	*Bison/Bos*	2.5	3.2	2015	MAMS-25516	40 800	620	-1.747
S-EVA 31801*	J3-3408	4	Middle Palaeolithic/Mousterian	*Bison/Bos*	1.3	3.2	2015	MAMS-25519	39 180	520	-1.628
S-EVA-29431	F7-136	3	Middle Palaeolithic/Mousterian	unknown	3.8	3.2	2014	MAMS-21194	45 280	820	-2.424
S-EVA-29433	F7-187	3	Middle Palaeolithic/Mousterian	unknown	4.3	3.2	2014	MAMS-21195	47 480	1060	-2.423
S-EVA-29436	F7-221	3	Middle Palaeolithic/Mousterian	unknown	3.0	3.2	2014	MAMS-21196	43 140	640	-2.305
S-EVA-29437*	F7-345	2	Middle Palaeolithic/Mousterian	unknown	4.1	3.2	2014	MAMS-21197	>49 000		-2.711

Isotopic values, C:N ratios, amount of collagen extracted (%Coll, >30 kDa fraction). The results of AMS radiocarbon dating of 40 samples from La Ferrassie. δ^{13}C values are reported relative to the vPDB standard, and δ^{15}N values are reported relative to the AIR standard. The bones with human modifications are indicated by an asterisk* in the MPI Lab Code. Results are rounded to the nearest 10 years. The outlier samples due to the wall effect are indicated with an • in the layer column.

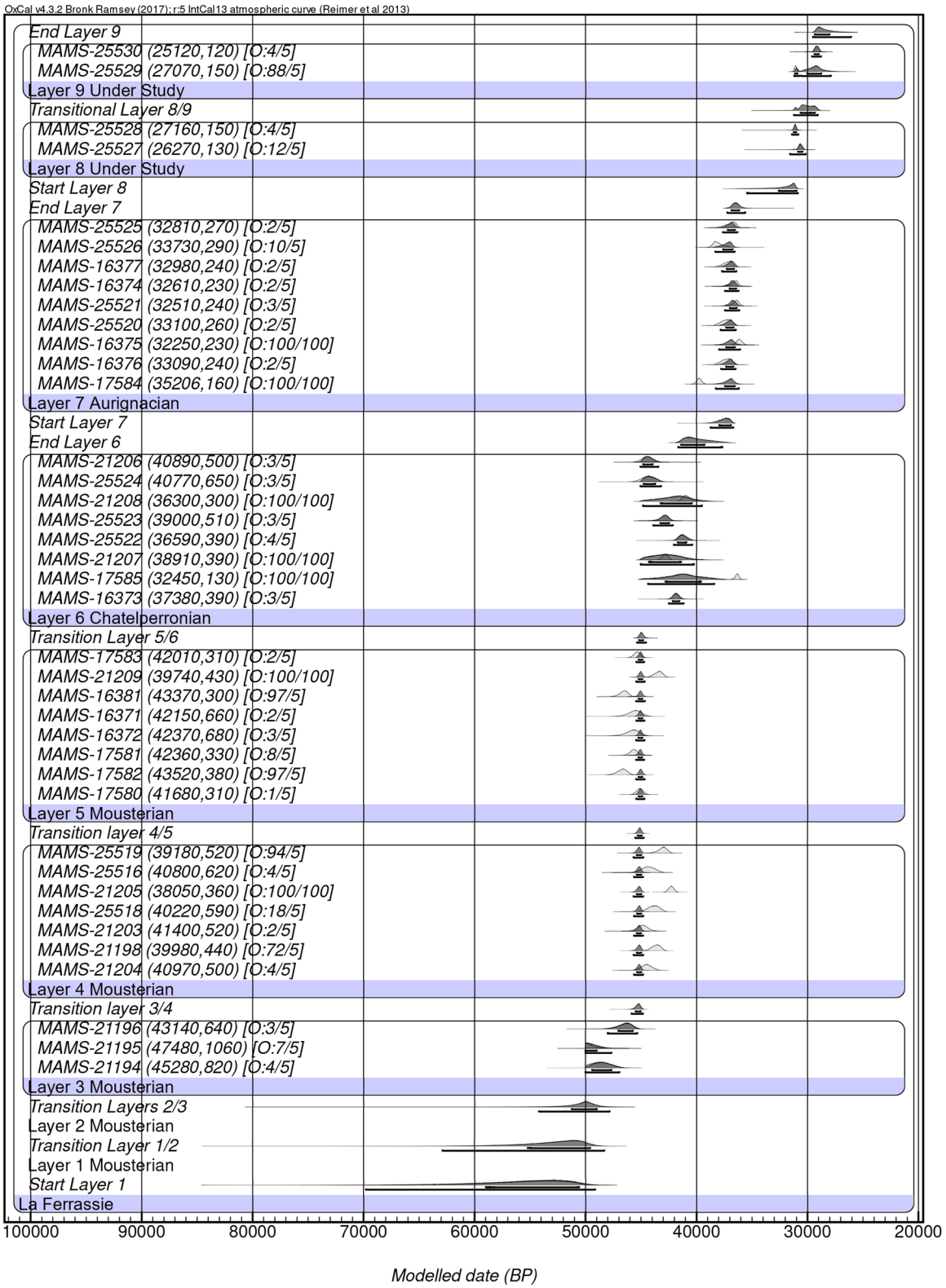

Figure 2. Bayesian Model 1 of La Ferrassie. Radiocarbon dates are calibrated using IntCal13 (Reimer *et al.*, 2013); the model and boundaries were calculated using OxCal 4.3, including a General t-type Outlier Model (Ramsey, 2009). Outliers' prior and posterior probabilities are shown in square parenthesis. Six samples are excluded from the model iterations by giving them a prior outlier probability of 100% because of the wall effect. [Color figure can be viewed at wileyonlinelibrary.com]

Archaeological sites used for regional comparison

Our goal here is to try to minimise the noise in reconstructing scenarios of the last Neanderthals and the appearance of *Homo sapiens* by investigating chronologically the sites that play a pivotal role in the late Middle to early Upper Palaeolithic period in France. Thus, we created a list of sites to which the criteria mentioned above were applied. This means that the radiocarbon pretreatment method is described in detail, the AMS laboratory number and isotopic values are indicated, and in the case of bones the C:N ratio and collagen yield are provided, along with well-described stratigraphic information and a good evaluation of the archaeological

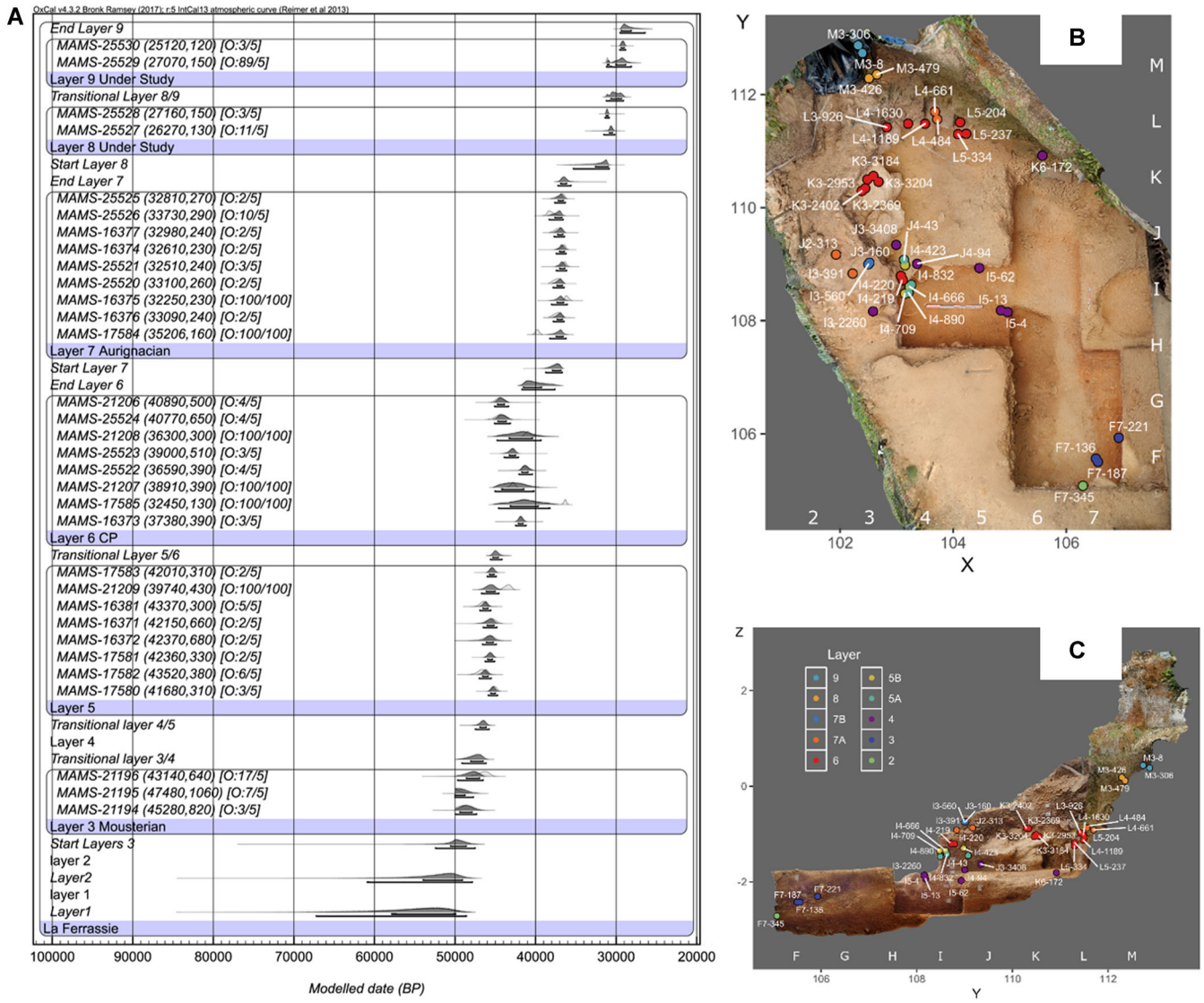

Figure 3. Bayesian Model 2 of La Ferrassie. (A) Radiocarbon dates are calibrated using IntCal13 (Reimer *et al.*, 2013); the model and boundaries were calculated using OxCal 4.3, including a General t-type Outlier Model (Ramsey, 2009). Outliers' prior and posterior probabilities are shown in square brackets. Six samples are excluded from the model iterations by giving them a prior outlier probability of 100% because of the wall effect. (B) and (C) Location of the radiocarbon samples projected on a sagittal profile looking west (C) and plan view (B). Samples are labelled with their field codes (Unit-ID). The excavation grid letters and numbers (which correspond to Fig. 1) are shown on the interior edge of each figure. Images are in both cases derived from the georeferenced, structure from motion, 3D models made at the end of the excavation project. [Color figure can be viewed at wileyonlinelibrary.com]

material (See SI for more details). Several other papers already propose specific criteria for establishing a ^{14}C date dataset for Palaeolithic sites (Waterbolk, 1971, Pettitt *et al.*, 2003, Banks *et al.*, 2013, Barshay-Szmidt *et al.*, 2018), and in proposing our list we note that this is a work in progress and that adding new sites and dates will probably improve or change the present scenario.

Results

Collagen quality control

The isotopic values and the C:N ratios of all of the collagen samples from La Ferrassie fall within the acceptable range of the evaluation criteria (van Klinken, 1999). The collagen yield is between 1.1% and 4.4% (Table 3), which is higher than the 1% minimum for an acceptable value (van Klinken, 1999). Together the isotopic values and the FTIR results show that the environmental conditions across the Western Sector at La Ferrassie were overall good for collagen preservation (Table 3, and Fig. S1). Based on these results, we can confirm the good quality of the collagen extracts, and on this basis, we see no reason to reject any of the resulting ages. However, as in any archaeological site, outliers are recognised only after obtaining the final radiocarbon ages. Here at La Ferrassie there are some present, and these are carefully discussed below.

Uncalibrated radiocarbon results

Uncalibrated radiocarbon dates are given in ^{14}C BP at 1 sigma error in Table 3. For all of the radiocarbon ages in the 50 to 25 ka cal BP interval, our 1 sigma errors are only a few hundred years. Layer 2 yielded a date of >49 000 ^{14}C BP. This age comes from a single cut-marked bone. For Layer 3 we dated three animal bones without human modifications and obtained ages ranging between 47 480 and 43 140 ^{14}C BP. Seven animal bones from Layer 4, six of which have cut marks, range from 41 400 to 38 050 ^{14}C BP. Eight dates were obtained from Layer 5. Half of these samples showed marks indicative of human modification. The ages range from 43 520 to 39 740 ^{14}C BP. Here we observe a clear age inversion; the Layer 5 ages

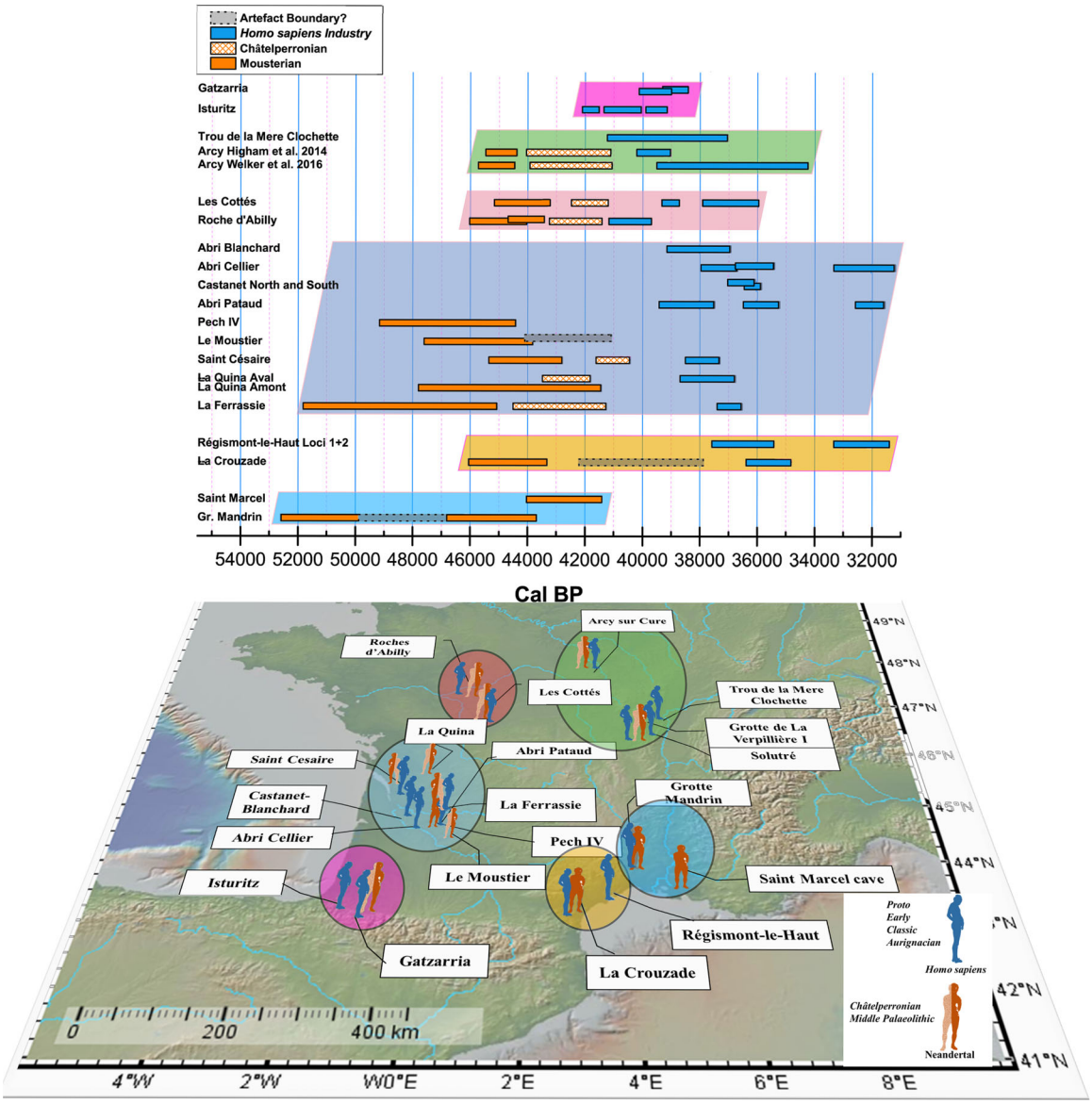

Figure 4. Regional chronological comparison. Chronological comparison of La Ferrassie with other French late Middle to early Upper Palaeolithic sites. The horizontal bars are the ranges produced from the 'date' command in OxCal (See SI for more details), except for the direct dates of humans in pink, which are the calibrated ranges. Upper Palaeolithic (*Homo sapiens*) layers are in blue, Middle Palaeolithic (Neandertals) are in orange, and the Châtelperronian (Neanderthals) in orange cross-hatching. The grey bars correspond to an 'artificial' boundary, probably imposed by the Bayesian model due to very poor sample selection or the absence of dates (empty phases). Since the diachronic succession between Protoaurignacian and Early Aurignacian is not always preserved in the sites selected, and the aim of the discussion is to reconstruct the dispersal of *Homo sapiens* across France, no differentiation in colours between different types of Aurignacian are displayed. All the bars represent 68.2% probability cal BP. The different coloured circles on the map are the different French areas discussed in the text. The colour of the circles in the map correspond to the colour of the squares in the graphic on top. [Color figure can be viewed at wileyonlinelibrary.com]

are older than the underlying Layer 4 ages. Eight animal bones were dated from the Châtelperronian Layer 6, three with cutmarks, yielding ages from 40 890 to 32 450 ^{14}C BP. The Aurignacian Layer 7 was sampled with nine bones, four of which have human modification marks, and yielded ages ranging from 35 210 to 32 250 to ^{14}C BP. Finally, two samples each for the top of the sequence (Layers 8 and 9) were dated to help with the archaeological attribution of Layer 8 and to help support an interpretation that, in fact, these layers derive from the upper cave situated just a few meters above the Western Sector. One of the bones from Layer 8 showed traces of human modification. The Layer 8 ages cluster together at 27 160 ± 150 and 26 270 ± 130 ^{14}C BP. The overlying Layer 9 produced one age that overlaps with Layer 8 (27 070 ± 150 ^{14}C BP) and a younger age of 25 120 ± 120 ^{14}C BP.

It was recognised that there is a potential taphonomic issue with seven of the samples. These samples were recovered from sediments adjacent to the limestone wall and could have been subject to vertical movement through the so-called wall effect. This taphonomic issue is rather common in cave sites where the movement of water along the cave walls can more easily displace artefacts. Additionally, the results show an age inversion in Layers 4 and 5 (both Middle Palaeolithic) with no obvious resolution. From the radiocarbon point of view, contamination from older carbon is an unlikely explanation for the older Layer 5 ages because the proportion of ^{14}C-free contamination required in this case would be 20%. Modern contamination of the younger Layer 4 ages is much more likely in this age range, but a) all of the samples passed the criteria for good quality collagen, b) all the samples were pretreated together with the control background bone, c) the pretreatment, as well as the sample selection was done in different years (from 2012 to 2015) and, last but not least, d) it is difficult to postulate a mechanism that would have contaminated only

the Layer 4 ages and in such a consistent way. With regard to this latter point, it is important to emphasise that the ages from Layers 4 and 5 show great internal consistency, both in terms of sample preparation and from a geological point of view. Moreover, the 22 samples that did not display human modifications have the same ^{14}C ranges like the one that did show human modification.

Alternatively, we can consider site formation processes to account for the Layers 4 and 5 radiocarbon discrepancies. One explanation could be that Layer 5 was originally deposited somewhere above its present location and was then, after the direct deposition of Layer 4 in the excavated area, redeposited on top of Layer 4 (See SI for detailed explanation). While such an explanation would account for the radiocarbon age inversion, there are, on the other hand, several arguments against this hypothesis. In fact, it is problematic to envision erosion that would selectively pick up deposits with a tight age constraint. It is also difficult to reconstruct a geologically reasonable scenario whereby the sediments of Layer 5 would have remained for ~2000 years in a location and then undergone erosion all at once, without being mixed with other deposits of different ages and types. Furthermore, the material found within Layer 5 in its current location is not decalcified or weathered as one might expect if it had been derived from previously deposited sediments from above, which were exposed and then reworked into the lower Western Sector area below.

However, Layer 4 will need further investigation before integrating its radiocarbon dates into the La Ferrassie model.

Bayesian model results

All ^{14}C ages were calibrated with the IntCal13 calibration curve (Reimer *et al.*, 2013) in the OxCal v4.3 (Ramsey, 2009). Calibrated dates and boundaries are given in Tables S2 and S3 in cal BP, with the 68.2% and 95.4% probability ranges. As mentioned above, we identified seven outliers that likely represent post-depositional movements. These were then excluded from both models (Model 1 and 2) by assigning a prior outlier probability of 100%. In Model 1, six more outliers, with a posterior probability higher than 15% were identified, showing once more the potential problem in Layer 4 (total of four outliers of seven samples, Table S2 and Fig. 2). Moreover, even if we do not consider the Agreement Index, due to the incorporation of the outlier Model, this is very low (4.8%), suggesting caution in interpreting the site's chronology. In this model, the boundaries, start and end, of Layer 4 range from 45 490 to 44 940 cal BP at 68.2% probability (Table 2). In Model 2, only two outliers, one in Layer 3 with posterior probability at 17% and one in Layer 9 with 90%, are identified (Table S3 and Fig. 2). In this case, the Agreement Index is 51.5%, and the boundaries of Layer 4 are significantly older than for Model 1 (48 060–46 130 cal BP at 68.2% probability). Although the boundaries of Layer 4 in Model 2 are considerably older than the one produced in Model 1, the differences between the boundaries for the various archaeological layers are only minor (See SI for more details). However, here, we consider Model 2 the better one for discussing the chronology of the site and placing the duration of the different archaeological divisions into a wider regional and continental context of other late Middle to Upper Palaeolithic sites and directly dated human fossils (Fig. 4). Layer 4 will need further investigation before integrating its radiocarbon dates into the La Ferrassie model (See SI for more details).

Discussion

Starting from the southeast of the region, at Grotte Mandrin and Saint Marcel the presence of Neanderthals is documented. The presence of *Homo sapiens* at Grotte Mandrin is documented only by the study of the lithic assemblage (Protoaurignacian) in Slimak *et al.* (2002, 2008, 2019), and no direct dates are provided. In Fig. 4, the Neronian transitional industry at Grotte Mandrin is coloured in grey because in the Bayesian model, provided by Higham *et al.* (2014), this phase corresponds to an empty phase (without any dates) (Higham *et al.*, 2014). This could lead to an 'artificial' boundary, and further chronological work on this site is needed. Not far from these two sites are Régismont-le-Haut and La Crouzade. La Crouzade displays an 'artificial' boundary in the Middle Palaeolithic layers. In the upper layers C7 and C6, attributed to the Middle Palaeolithic, the dates reported are from ESR-U/Th (Saos *et al.*, 2019), with wide error ranges that do not provide precise details about the late occurrence of Neanderthals at the site. The date of the Aurignacian layer at La Crouzade comes from two samples. One of these is a direct dating of the La Crouzade IV human bone (R_Combine (OxA-X-2635-38 + ERL-9415) ^{14}C age 31 054 ± 340 BP). As mentioned in Saos *et al.* (2019), this date could be affected by contamination from younger carbon and additional dating is needed (See SI for more details).

For southwest France, we have included a substantial number of sites with Neanderthal and *Homo sapiens* remains. La Ferrassie is one of these. So far, the Châtelperronian at La Ferrassie is the earliest example of this industry in the region, appearing ca. 400 years before it shows up at Grotte du Renne (Arcy-sur-Cure) and Le Moustier (44 490–41 250 cal BP at 68.2% probability). The Châtelperronian of Layer K at Le Moustier shows a slight chronological overlap (ca. 270 years) with the Mousterian in Layer J (Gravina and Discamps, 2015). This could be an artificial boundary since this range is based only on one thermoluminescence date with a high error range (See SI for more details). At La Quina there are two sectors: La Quina Amont, which has only Middle Palaeolithic deposits, recently dated by OSL and ^{14}C by Frouin *et al.* (2017b), and La Quina Aval, which contains only Châtelperronian and Aurignacian. The La Quina Aval Châtelperronian dates are provided by Higham *et al.* (2014), and the Aurignacian is discussed in Verna *et al.* (2012). The age range of the La Quina Aval Châtelperronian is in the age range of the latest Middle Palaeolithic at La Quina Amont. This needs further study. Even if the Châtelperronian Level EJOP sup at Saint Césaire is considered a mixture of Middle Palaeolithic and Châtelperronian artefacts (Gravina *et al.*, 2018), the time span of the Châtelperronian/Middle Palaeolithic there overlaps with the Châtelperronian at La Ferrassie, Roche d'Abilly, Les Cottés and Grotte du Renne at Arcy-sur-Cure. Moreover, the calibrated age range of the Neanderthal skeleton at Saint Césaire encompasses the Châtelperronian Neanderthal bone from Grotte du Renne.

In this southwest region of France, there are also several sites that have only yielded assemblages made by *Homo sapiens* (Abri Pataud, Castanet, Abri Cellier, and Abri Blanchard). Abri Pataud is represented by the Early Aurignacian, evolved Aurignacian and the Gravettian (Higham *et al.*, 2011). At Abri Cellier, the upper part of the sequence is represented by an Aurignacian but of an uncertain type (White *et al.*, 2018). Some of these phases overlap with Castanet, Abri Blanchard and Abri Pataud. It is clear that in all of these sites there is no chronological overlap between Neanderthals and *Homo sapiens*. North of La Ferrassie, the Neanderthals from Roche d'Abilly and Les Cottés are of similar age. Both sites were

inhabited by Neanderthals and *Homo sapiens*, but during the ca.1500-year period of Aurignacian occupation at Roche d'Abilly there was no apparent occupation of Les Cottés. The first appearance of *Homo sapiens* at Les Cottés seems to be represented by the appearance of the Protoaurignacian some ~400 years later than at Roche d'Abilly. The direct date of the Neanderthal remain at Les Cottés is connected to a layer attributed to the Middle Palaeolithic.

For the northeast, we have included Grotte du Renne at Arcy-sur-Cure. At this site, the two models from Welker *et al.* (2016) and Higham *et al.* (2014) indicate an overlap for the Middle Palaeolithic and Châtelperronian occupations, but there is a significant difference in the time span of the Protoaurignacian. The duration of the Protoaurignacian at Grotte du Renne (Welker *et al.*, 2016) encompasses the Early Aurignacian from the neighbouring sites of Trou de la Mere Clochette-TMC, Grotte de la Verpillière I, and Solutré. This situation at Grotte du Renne could be seen as a palimpsest of Proto- and Early Aurignacian as already mentioned in Hublin *et al.* (2012). Figure 4 does not include dates for Grotte de la Verpillière I and Solutré (Floss *et al.*, 2015) because there are very few dates for these sites, and these dates were estimated long ago. However, they are important sites in the area, especially for the well documented Châtelperronian (Floss *et al.*, 2016) (see the map in Fig. 4) and, as mentioned in Floss *et al.* (2015), a new ^{14}C and ESR dating programme is underway. At Trou de la Mère Clochette the age range for Unit C (Proto- and Early Aurignacian) is based only on two radiocarbon dates (Szmidt *et al.*, 2010). The bar for Trou de la Mère Clochette in Fig. 4 represents Unit C, but obviously more dates are required.

From Fig. 4 it is clear that the Châtelperronian from the northern and central parts of France overlaps with the Protoaurignacian at Isturitz in the extreme southwestern part of the Aquitaine region (Barshay-Szmidt *et al.*, 2018). This situation suggests an overlap between Neanderthals and *Homo sapiens* of ca. 1600 years. We note that some question whether the Protoaurignacian can be exclusively attributed to *Homo sapiens* (Zilhão *et al.* 2015) and that the chronology at Isturiz is also questioned (more in the SI). All of the *Homo sapiens* assemblages seem contemporaneous except at Roche d'Abilly, Trou de la Mère Clochette, and Isturitz, which are among the oldest. Slimak (2019) states that the Protoaurignacian at Grotte Mandrin is among the oldest currently recorded in Europe, but no dates are available. This site is on a potential corridor of dispersal for *Homo sapiens* through to the western Mediterranean, which could explain the earlier dates at Isturitz. More chronological work is required for this important site.

Conclusion

In sum, the excellent state of collagen preservation in the La Ferrassie bones and the application of high-resolution sampling for radiocarbon dating have allowed us to refine the chronology of the site and have indicated that currently, the earliest appearance of the Châtelperronian is at La Ferrassie. At a regional scale, determining if, and to what extent, there was an overlap between Neanderthals and *Homo sapiens* based only on ^{14}C dates is made difficult by a number of issues: 1) the wide confidence intervals on the ^{14}C dates themselves; 2) having very few dates representative of individual phases; and 3) the limited precision of the calibration curve in this time range. Ongoing work on this third issue (Adolphi *et al.*, 2017; Muscheler *et al.*, 2014; Cheng *et al.*, 2018) will help to improve our understanding of the Middle to Upper Palaeolithic transition on a regional basis. For now, it seems that the chronological and the spatial sequences of the last Neanderthals in France progress from the southeast through the centre and to the northeast. On the other hand, while there are some data consistent with the arrival of *Homo sapiens* along a southern route parallel to the Mediterranean, more reliable dates from several key sites are required. At the moment, the earliest appearance of *Homo sapiens* in France is in the southwest corner without any clear indication of which route they took. If we accept that the dates for Isturitz are all valid then Neanderthals and *Homo sapiens* did overlap for about 1600 years in France. Furthermore, we are able to demonstrate that this overlap is not within individual sites or at even at neighbouring sites.

Supporting information

Additional supporting information may be found in the online version of this article at the publisher's web-site.

Figure S1. FTIR spectra of extracted collagen samples from different layers. All samples show the three major characteristic collagen peaks at a) 1655 cm^{-1} (amide I), b) 1548 cm^{-1} (amide II) and 1452 cm^{-1} (amino acid proline absorption). No additional peaks are observed.

Table S2. Bayesian Modelled calibrated ages and Boundaries of Model 1 provided by the IntCal13 using OxCal 4.3 program (Reimer et al., 2013, Ramsey, 2009). In red are the six samples, which are excluded from the model iterations by giving them a prior outlier probability of 100%.

Table S3. Bayesian Modelled calibrated ages and Boundaries of Model 2 provided by the IntCal13 (Reimer et al., 2013) using OxCal 4.3 (Ramsey, 2009). In red are the six samples, which are excluded from the model iterations by giving them a prior outlier probability of 100%. For a figure of the sequences, see Fig. 2 in the main text.

Acknowledgements. We are indebted to Lysann Rädisch, Annabell Reiner and Sven Steinbrenner of the Department of Human Evolution at the MPI-EVA for technical assistance. We want to acknowledge the Max Planck Society, Service Régional de l'Archéologie, Conseil Général de Dordogne, the National Science Foundation, and the Leakey Foundation for funding the excavation and analysis of La Ferrassie. This study received additional financial support from the Région Aquitaine (through the CHROQUI programme) and the LaScArBx Labex (Project number ANR-10-LABX-52). S. Talamo is supported by the European Research Council under the European Union's Horizon 2020 Research and Innovation Programme (grant agreement No. 803147-951 RESOLUTION, https://site.unibo.it/resolution-erc/en). We note that Harold Dibble participated fully in the research presented here and was able to comment on a nearly final version of the manuscript. The La Ferrassie team misses him greatly. Finally, we thank the editor, Joao Zilhão and the other two anonymous reviewers for their critical reading, whose suggestions helped improve and clarify this manuscript. Open access funding enabled and organized by Projekt DEAL.

Author contributions—The dating project was conceived by S.T., S.J.P.M. and J-J. H. The LF project was conceived by A.T. in cooperation with H.L.D., D.S., S.J.P.M., P.G. and V.A. The sample selection for radiocarbon dating was performed by S.T. and T.E.S.

S.T. analysed the isotopic values, the AMS results and built the different OxCal models. V.A. and P.G. studied the geology and microstratigraphy. R.M. performed FTIR analysis. S.M. and T.E.S. performed the faunal analysis. All the authors discussed the results and contributed to the Supplementary Information. S.T. wrote the paper with contributions from all co-authors.

Additional information

Supplementary information accompanies this paper at wileyonlinelibrary

Competing financial interests: The authors declare no competing financial interests.

Data availability statement

The data that support the findings of this study are available in the supplementary material of this article.

References

Adolphi F, Muscheler R, Friedrich M *et al*. 2017. Radiocarbon calibration uncertainties during the last deglaciation: Insights from new floating tree-ring chronologies. *Quaternary Science Reviews* **170**: 98–108.

Aldeias V, Goldberg P, Sandgathe D *et al*. 2014. Insights into Site Formation Processes of the Middle and Upper Paleolithic Layers in the Western Section of La Ferrassie (Dordogne). In *Proceedings of the 4th Annual Meeting of the European Society for Human Evolution* (ESHE).

Banks WE, D'Errico F, Zilhão J. 2013. Revisiting the chronology of the Proto-Aurignacian and the Early Aurignacian in Europe: A reply to Higham *et al*.'s comments on Banks *et al*. *Journal of Human Evolution* **65**: 810–817.

Barshay-Szmidt C, Normand C, Flas D *et al*. 2018. Radiocarbon dating the Aurignacian sequence at Isturitz (France): Implications for the timing and development of the Protoaurignacian and Early Aurignacian in western Europe. *Journal of Archaeological Science: Reports* **17**: 809–838.

Bertran P, Caner L, Langohr R *et al*. 2008. Continental palaeoenvironments during MIS 2 and 3 in southwestern France: the La Ferrassie rockshelter record. *Quaternary Science Reviews* **27**: 2048–2063.

Bordes F. 1961. Mousterian Cultures in France. *Science* **134**: 803–810.

Brock F, Bronk Ramsey C, Higham T. 2007. Quality assurance of ultrafiltered bone dating. *Radiocarbon* **49**: 187–192.

Brown TA, Nelson DE, Vogel JS *et al*. 1988. Improved Collagen Extraction by modified Longin method. *Radiocarbon* **30**: 171–177.

Cheng H, Edwards RL, Southon J *et al*. 2018. Atmospheric 14C/12C changes during the last glacial period from Hulu Cave. *Science* **362**: 1293.

D'Elia M, Gianfrate G, Quarta G *et al*. 2007. Evaluation of possible contamination sources in the ^{14}C analysis of bone samples by FTIR spectroscopy. *Radiocarbon* **49**: 201–210.

De Sonneville-Bordes D. 1960. Le paléolithique supérieur en Périgord, (Vol. 1). Delmas.

Delibrias G. 1984. La datation par le carbone 14 des ossements de la Ferrassie. H. Delporte (éd.). *Le Grand Abri de La Ferrassie, Etudes Quaternaire 7*, pp. 105–107.

Delporte H. 1984. *L'Aurignacien de la Ferrassie. In Le Grand Abri de La Ferrassie*. Delporte H (ed.). Études Quaternaires, Paris 7, pp. 145–234.

Delporte H, Delibrias G. 1984. *Le grand abri de La Ferrassie: fouilles 1968-1973*, Etudes Quaternaires n°7, Laboratoire de Paléontologie Humaine, Paris.

Dibble HL, Lin SC, Sandgathe DM *et al*. 2018. Assessing the Integrity of Older Archeological Collections: an Example from La Ferrassie. *Journal of Paleolithic Archaeology* **1**: 179–201.

Djindjian F. 1986. Recherches sur l'Aurignacien du Périgord à partir des données nouvelles de La Ferrassie. *L'Anthropologie (Paris)* **90**: 89–106.

Floss H, Hoyer C, Würschem H. 2016. Le Châtelperronien de Germolles (Grotte de La Verpillière I, commune de Mellecey, Saône-et-Loire, France). *PALEO. Revue d'archéologie préhistorique*, **27** 149–176.

Floss H, Hoyer CT, Heckel C *et al*. 2015. The Aurignacian in Southern Burgundy. Palethnologie, Archéologie et sciences humaines, (7).

Frouin M, Guérin G, Lahaye C *et al*. 2017a. New luminescence dating results based on polymineral fine grains from the Middle and Upper Palaeolithic site of La Ferrassie (Dordogne, SW France). *Quaternary Geochronology* **39**: 131–141.

Frouin M, Lahaye C, Valladas H *et al*. 2017b. Dating the Middle Paleolithic deposits of La Quina Amont (Charente, France) using luminescence methods. *Journal of Human Evolution* **109**: 30–45.

Fu Q, Hajdinjak M, Moldovan OT *et al*. 2015. An early modern human from Romania with a recent Neanderthal ancestor. *Nature* **524**: 216–219.

Goldberg P, Aldeias V, Balzeau A *et al*. 2016. On the context of the Neanderthal Skeletons at La Ferrassie: new evidence on old data. In *Annual Meeting the European Society for the Study of Human Evolution, Madrid*.

Gómez-Olivencia A, Crevecoeur I, Balzeau A. 2015. La Ferrassie 8 Neandertal child reloaded: New remains and re-assessment of the original collection. *Journal of Human Evolution* **82**: 107–126.

Gravina B, Discamps E. 2015. MTA-B or not to be? Recycled bifaces and shifting hunting strategies at Le Moustier and their implication for the late Middle Palaeolithic in southwestern France. *Journal of Human Evolution* **84**: 83–98.

Gravina B, Bachellerie F, Caux S *et al*. 2018. No Reliable Evidence for a Neanderthal-Châtelperronian Association at La Roche-à-Pierrot, Saint-Césaire. *Scientific Reports* **8** 15134.

Guérin G, Frouin M, Talamo S *et al*. 2015. A multi-method luminescence dating of the Palaeolithic sequence of La Ferrassie based on new excavations adjacent to the La Ferrassie 1 and 2 skeletons. *Journal of Archaeological Science* **58**: 147–166.

Higham T. 2011. European Middle and Upper Palaeolithic radiocarbon dates are often older than they look: problems with previous dates and some remedies. *Antiquity* **85**: 235–249.

Higham TFG, Jacobi RM, Bronk Ramsey C. 2006. AMS radiocarbon dating of ancient bone using ultrafiltration. *Radiocarbon* **48**: 179–195.

Higham T, Jacobi R, Basell L *et al*. 2011. Precision dating of the Palaeolithic: A new radiocarbon chronology for the Abri Pataud (France), a key Aurignacian sequence. *Journal of Human Evolution* **61**: 549–563.

Higham T, Douka K, Wood R *et al*. 2014. The timing and spatiotemporal patterning of Neanderthal disappearance. *Nature* **512**: 306–309.

Hublin J-J. 2015. The modern human colonization of western Eurasia: when and where? *Quaternary Science Reviews* **118**: 194–210.

Hublin J-J, Talamo S, Julien M *et al*. 2012. Radiocarbon dates from the Grotte du Renne and Saint-Césaire support a Neandertal origin for the Châtelperronian. *PNAS* **109**: 18743–18748.

Hublin J-J, Sirakov N, Aldeias V *et al*. 2020. Initial Upper Palaeolithic Homo sapiens from Bacho Kiro Cave, Bulgaria. *Nature* **581**(7808): 299–302.

Korlević P, Talamo S, Meyer M. 2018. A combined method for DNA analysis and radiocarbon dating from a single sample. *Scientific Reports* **8**: 4127.

Longin R. 1971. New method of collagen extraction for radiocarbon dating. *Nature* **230**: 241–242.

Mellars PA, Bricker HM, Gowlett JAJ *et al*. 1987. Radiocarbon Accelerator Dating of French Upper Palaeolithic Sites. *Current Anthropology* **28**: 128–133.

Muscheler R, Adolphi F, Knudsen MF. 2014. Assessing the differences between the IntCal and Greenland ice-core time scales for the last 14,000 years via the common cosmogenic radionuclide variations. *Quaternary Science Reviews* **106**: 81–87.

Pettitt PB, Davies W, Gamble CS *et al*. 2003. Palaeolithic radiocarbon chronology: quantifying our confidence beyond two half-lives. *Journal of Archaeological Science* **30**: 1685–1693.

Peyrony D. 1934. La Ferrassie: Moustérien, Périgordien, Aurignacien. Préhistoire III, pp. 1–92.

Ramsey CB. 2009. Dealing with outliers and offsets in radiocarbon dating. *Radiocarbon* **51**: 1023–1045.

Reimer PJ, Bard E, Bayliss A *et al*. 2013. IntCal13 and Marine13 Radiocarbon Age Calibration Curves 0–50,000 Years cal BP. *Radiocarbon* **55**: 1869–1887.

Ruebens K, Mcpherron SJP, Hublin J-J. 2015. On the local Mousterian origin of the Châtelperronian: Integrating typo-technological, chronostratigraphic and contextual data. *Journal of Human Evolution* **86**: 55–91.

Saos Thibaud, Grégoire Sophie, Bahain Jean-Jacques, Higham Thomas, Moigne Anne-Marie, Testu Agnès, Boulbes Nicolas, Bachellerie Manon, Chevalier Tony, Becam Gaël, Duran Jean-Pierre, Alladio Alex, Ortega Maria Illuminada, Devièse Thibaut, Shao Qingfeng (2019) The Middle and Upper Palaeolithic at La Crouzade cave (Gruissan, Aude, France): New excavations and a chronostratigraphic framework. *Quaternary International*, http://doi.org/10.1016/j.quaint.2019.11.040

Slimak L. 2008. The Neronian and the historical structure of cultural shifts from Middle to Upper Palaeolithic in Mediterranean France. *Journal of Archaeological Science* **35**: 2204–2214.

Slimak L. 2019. For a cultural anthropology of the last Neanderthals. *Quaternary Science Reviews* **217**: 330–339.

Slimak L, Pasesse D, Giraud Y. 2002. La grotte Mandrin et les premières occupations du Palèolithique supérieur en Occitanie orientale. Bon F, Maillo Fernandez JM, Ortega Cobos D (eds). Autour des Concepts de Protoaurignacien, d'Aurignacien Initial et Ancien: Unité et Variabilité des Comportements Techniques des Premiers Groupes d'Hommes Modernes dans le Sud de la France et le Nord de l'Espagne. *Proceedings of the round table held in Toulouse 27 Feb. – 1 March 2003, Espacio, Tiempo y Forma, serie I, Prehistoria y Arqueologia, Université de Toulouse le Mirail, Universidad de Girona, Universidad*,15, 237–259.

Smirnov Y. 1989. Intentional human burial: Middle Paleolithic (last glaciation) beginnings. *Journal of World Prehistory* **3**: 199–233.

Szmidt CC, Brou L, Jaccottey L. 2010. Direct radiocarbon (AMS) dating of split-based points from the (Proto)Aurignacian of Trou de la Mère Clochette, Northeastern France. Implications for the characterization of the Aurignacian and the timing of technical innovations in Europe. *Journal of Archaeological Science* **37**: 3320–3337.

Talamo S, Richards M. 2011. A comparison of bone pretreatment methods for AMS dating of samples >30, 000 BP. *Radiocarbon* **53**: 443–449.

Texier J-P 2006. In *Sédimentogenèse de Sites Préhistoriques Classiques du Périgord*. Texier J-P, Kervazo B, Lenoble A *et al* (eds). Pôle International de la Préhistoire, Les Eyziies, 2006. http://pole-prehistoire.com/v4/images/PDF/sedimento.pdf

Turq A, Dibble HL, Goldberg P *et al*. 2012. Reprise des fouilles dans la partie ouest du gisement de la Ferrassie, Savignac-de-Miremont, Dordogne: problématique et premiers résultats. In *Quaternaire continental d'Aquitaine: un point sur les travaux récents Quaternaire Continental d'Aquitaine, excursion AFEQ - ASF 2012*, Bertran P, Lenoble A (eds). Association des Sedimentologistes Francais: France.

van Klinken GJ. 1999. Bone Collagen Quality Indicators for Palaeodietary and Radiocarbon Measurements. *Journal of Archaeological Science* **26**: 687–695.

Verna C, Dujardin V, Trinkaus E. 2012. The Early Aurignacian human remains from La Quina-Aval (France) Original Research Article. *Journal of Human Evolution* **62**: 605–617.

Waterbolk HT. 1971. Working with radiocarbon dates. *Proceedings of the Prehistoric Society* **37**: 15–33.

Welker F, Hajdinjak M, Talamo S *et al*. 2016. Palaeoproteomic evidence identifies archaic hominins associated with the Châtelperronian at the Grotte du Renne. *Proceedings of the National Academy of Sciences* 113: 11162–11167.

White R, Bourrillon R, Mensan R *et al*. 2018. Newly discovered Aurignacian engraved blocks from Abri Cellier: History, context and dating. *Quaternary International* **498**: 99–125.

Yizhaq M, Mintz G, Cohen I *et al*. 2005. Quality controlled radiocarbon dating of bones and charcoal from the early prepottery neolithic B (PPNB) of Motza (Israel). *Radiocarbon* **47**: 193–206.

Zilhão J. 2016. Lower and Middle Palaeolithic Mortuary Behaviours and the Origins of Ritual Burial. In *Death rituals, social order and the archaeology of immortality in the ancient world*, Renfrew C, Boyd MJ, Morley I (eds). Cambridge University Press: Cambridge. pp. 27–44.

Zilhão J, Banks W, D'Errico F. 2015. Is the Modern vs. Neanderthal dichotomy appropriate any longer for the technocomplexes of the Middle-to-Upper Paleolithic transition. In *Proceedings of the 5th Annual Meeting of the European Society for Human Evolution (ESHE)*.

